

## STRONG GROUND MOTION SIMULATION OF 2017 EARTHQUAKE IN KHORASAN-RAZAVI, IRAN

Hesaneh MOHAMMADI

*Ph.D. Student, Geophysics Department, Tehran North Branch, Islamic Azad University, Tehran, Iran*  
*h.mohammadi@iau-tnb.ac.ir*

Maryam SEDGHI

*Ph.D. Student, Geophysics Department, Tehran North Branch, Islamic Azad University, Tehran, Iran*  
*maryamsedghi@ndri.ir*

Mohammad Reza GHEITANCHI

*Professor, Institute of Geophysics, University of Tehran, Tehran, Iran*  
*mrghchee@ut.ac.ir*

**Keywords:** Strong ground motion, Source parameters, Rupture characteristics, Empirical Green Function, Stochastic finite-fault method

On April 5, 2017, an earthquake with moment magnitude of 6.1 occurred 80 km southeast of Mashhad city in Khorasan-Razavi province (Sefid Sang earthquake). In this paper, in order to estimate source parameters and rupture process of the earthquake, the Empirical Green Function (EGF) method and the stochastic finite-fault (SFF) technique were applied to simulate strong ground motion. These techniques permit estimation of parameters such as seismic moment, corner frequency, and source duration and rupture characteristics of the earthquake (Miyake et al., 2000). These methods have been widely used in Iran to simulate earthquakes in different regions such as 2005 Zarand earthquake by Zafarani (2012), 2004 Firozabad Kojoor earthquake by Rahimi-Bahoosh and Hamzehloo (2011).

To simulate the earthquake by EGF method, the focal mechanism of the element (small) event should be similar to that of the target (main) event (Irikura, 1991), so that the aftershock ( $M_w=4.8$ ) was used as the empirical Green function, has the focal mechanism (Strike:  $304^\circ$  Dip:  $49^\circ$ , Rake:  $134^\circ$ ) similar to that of the main event (Strike:  $329^\circ$  Dip:  $45^\circ$ , Rake:  $127^\circ$ ). In this technique, the main shock fault plane is divided into sub faults of equal size. The size of the main fault and sub faults corresponds to the rupture area of main event and small event, respectively. In this study, the fault rupture dimensions were calculated using the equations estimated by Wells and Coppersmith (1994). In this study, near-source data recorded by 19 accelerometers were used to estimate source parameters. Before using accelerograms, data processing is necessary; it includes baseline correction and filtering. By a linear correction, the divergence from the base line was resolved; also by 4th order of Butterworth filter the data were filtered, this filtering helped baseline correction too. The stochastic simulation technique developed by Motazedian and Atkinson (2005) is also employed in this study. This method requires a detailed knowledge of the path and site effects; Input parameters are based on the characteristics of both the source and the path (seismic velocities and attenuation in the crust). The path attenuation is quantified by the quality factor, Q-value, and geometric spreading function. In this study, the quality factor Evaluated in this region by Shanaki et al. (2011) was used. The modeling considers shear-wave velocity, Crustal Density, Rupture propagation speed, fault-rupture dimensions, focal mechanism, seismic moment or magnitude, stress drop, slip distribution, hypocentral distance (or epicentral distance), focal depth, and fault pulsing percentage. The stress drop controls the amplitudes of high frequency radiation while the fault pulsing percentage influences the relative amount of low frequency radiation (Motazedian and Atkinson, 2005). At high frequencies, the acceleration spectral amplitude decreases rapidly; this has been modeled with the spectral decay factor  $\kappa$ . Its site component,  $\kappa_0$ , is used here as input parameter. After simulating the earthquake applying EGF and SFF methods; the observed records and the simulated graphs by these two techniques, were compared. We present the results of the simulations and their comparisons with the observed Fourier and Response spectra of the earthquake in Figure 1. Also, the peak values of the observed and simulated records of the main event in Torbat-e-Jam station are shown in Table 1. The stochastic simulation method is effective at predicting ground motions



from a large earthquake, especially for regions where the absence of small magnitude event records precludes the application of the EGF method. We tested the technique by comparing the synthetic and the recorded motion from the Sefid-Sang earthquake ( $M_w=6.1$ ). The comparison suggests that this method is effective at simulating near-source ground motions in a broad-frequency range of engineering interest. However, the results achieved from applying EGF method have better agreement with the observed ones; since records of small earthquakes used as empirical Green functions inherently include propagation and site effects, so that uncertainties associated with the crustal structure and local geology are eliminated (Hartzell, 1978, 1992). In general, the synthetics are in good agreement with observations in almost all cases, considering inherent limitations of the methods and their simplicity.

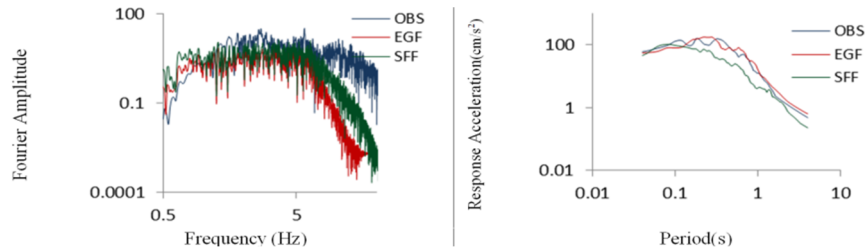


Figure 1. Observed and synthetic Fourier and acceleration response spectra of the main event in L component of Torbat-e-Jam station.

Table 1. The peak Ground Acceleration (PGA)/ Velocity (PGV) / displacement (PGD) and the duration of the observed and simulated diagrams of the earthquake in three components.

Station	Parameter	Observed			Synthetic(SFF)	Synthetic(EGF)		
		L	T	V		L	T	V
Torbat-e-Jam	PGA( $\text{cm/s}^2$ )	63.02	55.16	32.15	52.14	63.16	55.36	29.12
	PGV( $\text{cm/s}^2$ )	3.20	2.17	1.24	0.92	3.59	3.06	1.15
	PGD( $\text{cm/s}^2$ )	0.19	0.14	0.07	0.04	0.20	0.17	0.08
	Duration(s)	16	17	24	9	13	14	21

The estimated fault plane solution shows reverse mechanism with strike-slip component for this event, the fault caused this earthquake is determined as a reverse oblique fault (mostly compressional with a small strike slip component with North West-South East fault trend). Considering the fault plane and distribution of aftershocks, the rupture initiated at the depth of 11 km and propagated from hypocenter from North West to South East direction. The duration of the rupture in this event was about more than 18 seconds. April 5, 2017 earthquake was one of the several events with magnitude greater than 6 that have occurred in this region, one seismic event at a distance close to or even in great cities such as Mashhad would cause massive destruction and loss of lives. Therefore, the ground motion characteristics during the earthquakes should be considered for the high safety design of the damaged area.

## REFERENCES

- Hartzell, S.H. (1992). Estimation of near-source ground motions from a teleseismically derived rupture model of the 1989 Loma Prieta, California earthquake. *Bulletin of the Seismological Society of America*, 82, 1991- 2013.
- Hartzel, S.H. (1978). Earthquake aftershocks as Green functions. *Geophys. Res. Letters*, 5, 1-4.
- Miyake, H., Iwata, T., and Irikura, K. (2000). Source characterization of Inland crustal earthquakes for near- source ground motions. *Proceedings of the 6<sup>th</sup> International Conference on Seismic Zonation*.
- Motazedian, D. and Atkinson, G.M. (2005). Stochastic finite-fault modeling based on a dynamic corner frequency. *Bull. Seismol. Soc. Am.*, 95, 995-1010.
- Rahimi-Bahoosh, H. and Hamzehloo, H. (2011). Simulation of strong ground motion for the 2004 Firozabad Kojoor earthquake in northern Iran. *Iranian Journal of Geophysics*, 5(3), 1-13.
- Shanaki, S., Gheitanchi, M.R., Abredari, H., and Miraj, K. (2011). Evaluation of quality factor beneath the local seismic network in NE Iran. *Journal of the Earth*, 6(21), 51-60.
- Wells, D. and Coppersmith, K. (1994). New empirical relationships among magnitude. Rupture length, rupture width, rupture area and surface displacement. *Bull. Seismol. Soc. Am.*, 8, 974-1002.
- Zafarani, H. (2012). A hybrid empirical-stochastic method for ground motion simulation; a sample study: the 22 February 2005 (MW 6.4) Zarand (Central Iran) earthquake. *15 WCEEAT, Lisbon, Portugalociety of America*, 82(1), 104-119.